Comptes rendus - Geoscience 351 (2019) 395–405

Contents lists available at ScienceDirect

Comptes rendus - Geoscience

www.journals.elsevier.com/comptes-rendus-geoscience

Tectonics, Tectonophysics

Variscan stress regime rotation: Insights from the analysis of kink folds in the northern margin of the Bohemian Massif, South Poland

Jerzy Żaba, Krzysztof Gaidzik*

Department of Fundamental Geology, Faculty of Earth Sciences, University of Silesia, Będzińska 60, 41-200 Sosnowiec, Poland

ARTICLE INFO

Article history:
Received 12 November 2018
Accepted 16 April 2019
Available online 18 June 2019
Handled by Isabelle Manighetti

Keywords:
Kink fold
Butterfly diagram
Structural evolution
Karkonosze
Bohemian Massif

ABSTRACT

We aimed to determine variations in stress regimes during the youngest Variscan deformations in the northern part of the Bohemian Massif. For this purpose, we calculated the orientation of the principal stress and strain axes for kink folds observed in the metamorphic envelope of the Karkonosze Granite, using two methods: 1) the traditional method, incorporating structural diagrams (for conjugate kink folds only), and 2) butterfly diagram analysis. The use of both methods enabled us to determine the stress regime, based not only on conjugate but also on monoclinal kink bands. The obtained results prove that butterfly diagram analysis, when applied to monoclinal kink folds, yields reliable results, especially when calibrated using the internal friction angle (Φ) calculated for the conjugate structures.

We identified two generations of kink folds: 1) an older one, developed under sub-latitudinal shortening and most probably related to the Early Carboniferous terminal stages of the northwest-directed thrusting of the metamorphic units, and 2) a younger one; produced by north-south Variscan Carboniferous compression, and the emplacement and subsequent doming of the Karkonosze Granite. This is the first study on brittle-ductile structures observed commonly in the metamorphic units of the Bohemian Massif, showing their relation to the granitoid intrusion and complementing the tectonic models that usually omit kink folds.

1. Introduction

Kink folds represent a distinct type of double-hinged fold marking the transition between ductile and brittle deformations. Worldwide examples show that they commonly represent the youngest fold structures in a specific area, produced during the late stages of deformation occurring in both metamorphic and, less frequently, sedimentary rocks (e.g., Behr, 1983; Dewey, 1965; Gaidzik and Żaba, 2017; Johnson and Manuszak, 2001; Julivert and Soldevila, 1998; MacKenzie et al., 2010; Rubinkiewicz, 2005), followed by products of brittle tectonics. Apart from their characteristic appearance in simple two-dimensional cross sections (e.g., Dewey, 1965), they exhibit a complex, curving, anastomosing, and intersecting geometry in the third dimension, i.e. on the foliation plane (e.g., Dunham and Crider, 2012; Kirschner and Teixell, 1996; Verbeek, 1978). Kink folds typically form in rock with dense planes of anisotropy (i.e. bedding, foliation, cleavage), as a result of bending with shear caused by contraction parallel (or nearly parallel) to those planes (Anderson, 1974; Reches and Johnson, 1976). It is commonly accepted that the relationship between kink folds and surfaces of more intensive shear stress (Anderson, 1974; Johnson, 1977) frequently

* Corresponding author.
E-mail addresses: jerzy.zaba@us.edu.pl (J. Żaba), krzysztof.gaidzik@us.edu.pl (K. Gaidzik).

https://doi.org/10.1016/j.crte.2019.04.003
1631-0713/

causes kink band formation to follow two conjugate surfaces, which are directed to the axis of the highest compression (σ_1) at an obtuse angle (Anderson, 1974). The most important conditions initiating formation of kink folds include (Anderson, 1974; Honea and Johnson, 1976; Reches and Johnson, 1976): 1) rock with dense planes of flat-parallel (stratified) anisotropy; 2) the occurrence of a local disturbance of bedding (foliation), which marks the place of a kink fold initiation due to the concentration of shear stress in the internal limb; 3) a large frictional force concordant with the anisotropy surface; 4) an angle between the highest principal stress axis (σ_1) and the surface of anisotropy in the outer limb of less than $45^\circ - \Phi/2$ (Φ – internal friction angle); 5) high surrounding pressure, restraining a dispersed flexural slip. Typically, palaeostress reconstruction for these structures employs standard structural diagram calculations based on conjugate forms (Anderson, 1974; Ramsay and Huber, 1987). The interpretation of the stress regime responsible for the formation of monoclinal kink bands is rather complicated and tentative; however, this should be resolved using butterfly diagram analysis (Johnson, 2000), calibrated based on conjugate forms that allows the reconstruction of the largest main principal stress axis (σ_1) from the geometrical parameters of kink folds and the internal friction angle (Φ).

In the Bohemian Massif, surprisingly, despite the abundance of metamorphic units with a plethora of rocks favorable for kink fold formation, the literature on these structures and their recognition is scanty, including only some remarks on kink folds in the metamorphic envelope of the Karkonosze Granite intrusion (Gaidzik, 2011; Gaidzik and Żaba, 2017; Żaba, 1984a; Żaba and Kuzak, 1988). Their abundance in the metamorphic rocks of this area affords an opportunity to study them in greater detail, potentially enabling a conclusion regarding their formation history. The main goal of this study is to determine the number of generations of kink folds existing in the northern metamorphic envelope of the Karkonosze Granite, and consequently define their kinematic features and stress regimes for each generation and establish their position in models of Variscan evolution of the northern part of the Bohemian Massif. On the other hand, we also aim to test the usage of butterfly diagram analysis in the palaeostress reconstruction for the monoclinal kink folds. To accomplish this, we calculated the orientation of principal stress and strain axes for each observed kink fold using two methods: 1) the traditional method, using structural diagrams (for conjugate kink folds only) and 2) butterfly diagram analysis (Johnson, 2000). The use of both methods enabled us to determine the stress regime responsible for definite kink fold generation, based not only on conjugate but also monoclinal kink bands. It also allowed us, together with the superposition analysis, to determine the position and role of the studied structures in the subduction–exhumation models of the northern part of the Bohemian Massif.

2. Study area

The Sudetes, located in southwestern Poland on the northeastern margin of the Bohemian Massif, represents the northeasternmost outcropping segment of the Central European part of the Variscan Orogen, commonly subdivided into the Moldanubian, Saxothuringian, Rhenohercynian, Moravo-Silesian, and Teplá-Barrandian zones, and the Lugian domain (Mazur et al., 2006) (Fig. 1). The Sudetes defines a composite tectonic collage that consists of a mosaic of structurally distinct units, affected by mostly Devonian to Carboniferous deformation and characterized by abrupt changes in the dominant structural trends (Aleksandrowski and Mazur, 2002; Mazur et al., 2006). This region extends between two WNW–ESE-trending major fault zones: 1) the Middle Odra Fault Zone in the northeast, and 2) the Elbe Fault Zone in the southwest The study area is located in the northern metamorphic envelope of the Karkonosze Granite in the Karkonosze–Izera Massif (KIM), in the western part of Sudetes (Fig. 1a and b). This unit is limited to the north by the Intra-Sudetic Fault (ISF), which exhibits multiphase activity since Late Devonian (Aleksandrowski et al., 1997) and separates the KIM from the Kaczawa Complex (Fig. 1b).

The KIM is composed of a number of structural Neoproterozoic–Palaeozoic metamorphic units, with late Variscan multistage Karkonosze Granite plutonic complex at its core (Fig. 1b). The late- to post-orogenic Karkonosze granite has been dated several times through the years, using different methods that have yielded various ages, ranging generally from ~312 to ~320 Ma (e.g., Kryza et al., 2014; Kusiak et al., 2014; Žák et al., 2013). Several lithostratigraphic and tectonic subdivisions have been proposed for the metamorphic series of the KIM (e.g., Aleksandrowski and Mazur, 2002; Gaidzik, 2011; Jeřábek et al., 2016; Majka et al., 2016; Mazur, 1995; Mazur et al., 2006; Żelaźniewicz and Aleksandrowski, 2008). In general, these are interpreted as a pile of nappes produced by Variscan thrusting. The classical division of those nappe units (Aleksandrowski and Mazur, 2002; Mazur, 1995; Mazur and Aleksandrowski, 2001; Mazur et al., 2006; Seston et al., 2000) was recently revised by Žáčková et al. (2010) who proposed a distinction of four major tectonic units (Jeřábek et al., 2016; Majka et al., 2016). The lowermost is a parautochthonous unit composed of Neoproterozoic to Upper Cambrian/Lower Ordovician Lusatian and Izera (meta)granitoids (Borkowska et al., 1980; Kröner et al., 2001; Oberc-Dziedzic et al., 2010; Oliver et al., 1993) with their Neoproterozoic–Lower Palaeozoic cover (the Jěstěd Unit; Chaloupský, 1989). The upper thrust sheets are divided into Lower, Middle, and Upper Allochthon. Lower Allochthon is composed predominantly of garnet-bearing mica schists with subordinate bodies of orthogneisses, quartzites, calcsilicate rocks, and marbles (Jeřábek et al., 2016). The Middle Allochthon comprises mostly garnet-free mica schists, phyllites and marbles with a high proportion of metavolcanics (Žáčková et al., 2010). The Upper Allochthon is composed of mafic and felsic intrusive and extrusive rocks with low intensity of deformation and medium pressure metamorphism – Leszczyniec Unit (Fig. 1b; Seston et al., 2000).

The KIM is usually interpreted as a Variscan subduction–accretionary complex related to southeastward subduction and underthrusting of the Saxothuringian plate (Mazur et al., 2006). It experienced subduction and blueschist facies metamorphism (~360 Ma), followed by collision, nappe stacking, and widespread greenschist

facies metamorphism (ca. 340 Ma). The gneisses and mica schists of the Izera-Kowary Unit are considered to represent the Early Palaeozoic continental crust of the Saxothuringian Basin (Franke and Żelaźniewicz, 2000; Mazur and Aleksandrowski, 2001) that was subjected to Variscan deformation in the collision zone, which extended along the southern and eastern rims of the Karkonosze–Izera Massif. The contractional event (D_1) associated with northwest-directed thrusting and progressive metamorphism took place at the turn of the Late Devonian/Early Carboniferous (ca. 360–340 Ma). – The Early Carboniferous ESE-directed extensional collapse (D2) completed with the emplacement of the Karkonosze Granite (~312 to ~320 Ma), synchronous with regional doming followed by the formation of the East Karkonosze flexure under east–west contraction (D_3) (Mazur, 1995; Mazur and Aleksandrowski, 2001).

The northern part of the KIM is built of various types of pre-Variscan granites, granitogneisses, and gneisses, along with mica schists and hornfels. Izera granites (metagranites) were produced during the Early Paleozoic (Cambrian–Ordovician) magmatism, as corroborated by the following isochron ages: 480–450 Ma, Rb–Sr method (the whole rock) (Borkowska et al., 1980) or 515–480 Ma, Pb–Pb and U–Pb method (zircon) (Kröner et al., 2001; Oberc-Dziedzic et al., 2010; Oliver et al., 1993). The Izera orthogneisses are predominantly the products of the deformation of Izera granite (Żaba, 1984b); their multiphase deformation, leading to the formation of fold structures of different generations, occurred in the period from the Older Paleozoic to the Older Carboniferous.

Neoproterozoic–Palaeozoic mica schists, commonly interpreted as the metamorphic envelope of the Izera granites (Mazur et al., 2006), build west–east parallel running belts among Izera gneisses (Fig. 1c): the Złotniki Lubańskie, Stara Kamienica, and Szklarska Poręba belts. These belts are cut by aplite, pegmatite, and lamprophyre veins related to the Karkonosze Granite. Mica schists of the Szklarska Poręba and, partly, the Stara Kamienica belt fell under the thermal influence of the Variscan granitoid intrusion, transformed into cordierite-andalusite-biotite hornfels (Borkowska, 1966; Żaba, 1979) at temperatures of 570–750 °C and pressures of approximately 4–7 kbar.

Metamorphic rocks of the KIM underwent multiphase ductile deformations leading to the development of 4- to 5-fold generations in mica schists and orthogneisses (e.g., Dziemiańczuk and Dziemiańczuk, 1982; Gaidzik and Żaba, 2017; Żaba, 1979, 1984a; Żaba and Kuzak, 1988), frequently connected with the activity of ductile and ductile/brittle shear zones (Aleksandrowski et al., 1997; Czapliński, 1998; Mazur and Kryza, 1996). These are as follows (Gaidzik and Żaba, 2017; Jeřábek et al., 2016; Żaba, 1984a): F_1 – tight, isoclinal folds of variable orientation, F_2 – upright, inclined, and overturned, usually asymmetric folds with common axial cleavage, F_3 – chevron, asymmetric folds, F_4 and F_5 – kink bands.

3. Methods and materials

Field observations and measurements of the main parameters of kink folds (i.e. spatial orientation of fold limbs, fold axis, fold axial surfaces; see Fig. 2a) were carried out at 13 sites (Fig. 1) located within the Szklarska Poręba and Stara Kamienica schist belts (Fig. 1c). Conjugate kink folds, together with monoclinal structures, were observed in seven of the selected sites, whereas in others only monoclinal forms were recorded (Fig. 1c).

3.1. Principal stress and strain axes

The orientation of the principal stress and strain axes was determined using structural diagram analysis based on the spatial orientation of two axial surfaces of conjugate kink folds (e.g., Ramsay and Huber, 1987). Accordingly, the resulting directions of stretching and shortening, along with the direction of the main tectonic stress axes (σ_1, σ_2, and σ_3), were compared with the results of the butterfly diagram analysis of the same fold structures. This kind of stress and strain analysis of more common monoclinal kink folds does not guarantee reliable results. Thus, to determine the largest main principal stress axis (σ_1) for those structures, we used butterfly diagram analysis exclusively (Johnson, 2000, Fig. 2b).

3.2. Butterfly diagram analysis

Butterfly diagram analysis can be a very useful tool in studies on kink folds, because it enables the orientation of the main principal stress axis (σ_1) to be determined, not only for conjugate kink folds, but also for monoclinal, which are generally much more common (Johnson, 2000). The method uses the following parameters of kink folds (Fig. 2) (Johnson, 2000; Johnson and Manuszak, 2001): θ_{UL} – ultimate locking angle, i.e. the obtuse angle between the inner and outer limbs of a kink fold (θ_{ULZ} – ultimate locking angle of Z-shaped folds; θ_{ULS} – of S-shaped folds), and internal friction angle (Φ). A butterfly diagram is presented as a Cartesian coordinate system in which locking angles (θ_{UL}) are marked on the abscissa and inclination angles (β) on the ordinate (angle of divergence of the orientation of the stress axis (σ_1) from the anisotropy plane in outer limbs). The "butterfly pattern" on a diagram is produced by the area of possible values of the internal friction angle (Φ). Values of this parameter are limited by the following formula (Collier, 1978): $45^\circ - \Phi/2$; Reches and Johnson (1976).

The diagram is a graphic method for solving two equations with two variables (Φ and β) (Collier, 1978; Reches and Johnson, 1976: 1) for an ultimate locking angle of S-shaped folds (θ_{ULS}) $-\ \theta_{ULS} = 90^\circ - \Phi + \beta$, where $\theta > 0$; and 2) for an ultimate locking angle of Z-shaped folds (θ_{ULZ}) $-\ \theta_{LZ} = -(90^\circ - \Phi) + \beta$, where $\theta < 0$.

A butterfly diagram for conjugate kink folds enables the calculation of both the internal friction angle (Φ) and the inclination angle (β) from the two ultimate locking angles (θ_{UL}). Contrastingly, for monoclinal kink folds, both values, Φ and θ_{UL}, are needed to determine the value of β. The value of the internal friction angle on the anisotropy surface for most rock types varies from 20 to 40° (Barton and Choubey, 1977). In this study for monoclinal kink folds, we used $\Phi = 40^\circ$, i.e. the value estimated from the analysis of conjugate kink folds.

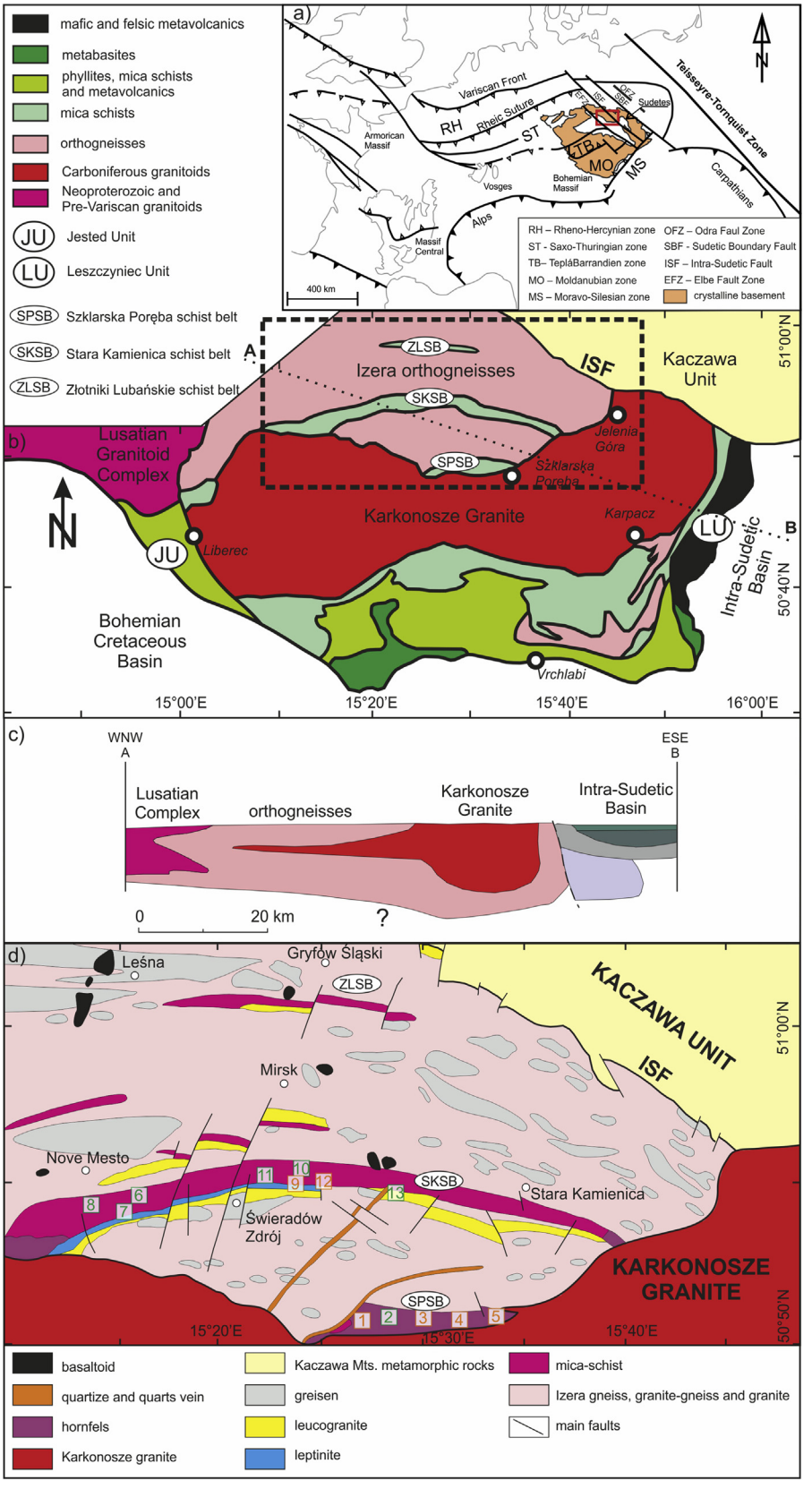
mafic and felsic metavolcanics
metabasites
phyllites, mica schists and metavolcanics
mica schists
orthogneisses
Carboniferous granitoids
Neoproterozoic and Pre-Variscan granitoids
JU Jested Unit
LU Leszczyniec Unit
SPSB Szklarska Poręba schist belt
SKSB Stara Kamienica schist belt
ZLSB Złotniki Lubańskie schist belt
a)
Variscan Front
Rheic Suture
RH
ST
TB
MO
MS
Armorican Massif
Vosges
Bohemian Massif
Massif Central
Alps
Carpathians
Teisseyre-Tornquist Zone
Sudetes
OFZ
SBF
ISF
EFZ
400 km
RH – Rheno-Hercynian zone
ST - Saxo-Thuringian zone
TB– TepláBarrandien zone
MO – Moldanubian zone
MS – Moravo-Silesian zone
OFZ – Odra Faul Zone
SBF - Sudetic Boundary Fault
ISF – Intra-Sudetic Fault
EFZ – Elbe Fault Zone
crystalline basement
b)
Lusatian Granitoid Complex
Izera orthogneisses
ISF
Kaczawa Unit
Jelenia Góra
Szklarska Poręba
Karkonosze Granite
Karpacz
Liberec
Intra-Sudetic Basin
Bohemian Cretaceous Basin
Vrchlabi
15°00'E
15°20'E
15°40'E
16°00'E
51°00'N
50°40'N
c)
WNW
ESE
Lusatian Complex
orthogneisses
Karkonosze Granite
Intra-Sudetic Basin
0
20 km
?
d)
Leśna
Gryfów Śląski
KACZAWA UNIT
ISF
Mirsk
Nove Mesto
Świeradów Zdrój
Stara Kamienica
KARKONOSZE GRANITE
15°20'E
15°30'E
15°40'E
51°00'N
50°50'N
basaltoid
quartize and quarts vein
hornfels
Karkonosze granite
Kaczawa Mts. metamorphic rocks
greisen
leucogranite
leptinite
mica-schist
Izera gneiss, granite-gneiss and granite
main faults

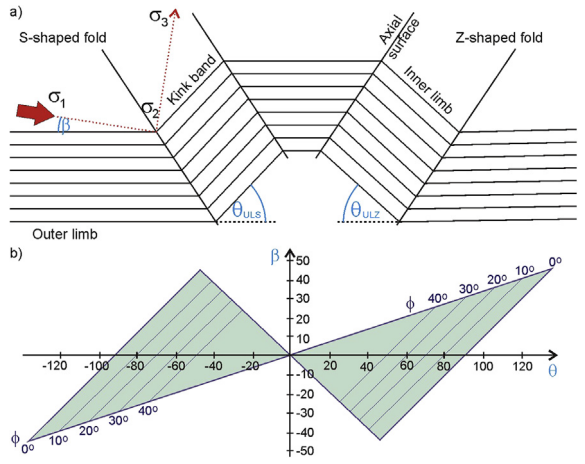

Fig. 2. a) Main parameters of a kink fold: $\sigma_1 > \sigma_2 > \sigma_3$ – main principal stress axes (maximum, neutral, and minimum, respectively); β – inclination angle, i.e. angle of divergence of the orientation of the stress axis (σ_1) from the anisotropy plane in outer limbs; θ_{ULZ} – ultimate locking angle of Z-shaped folds; θ_{ULS} – ultimate locking angle of S-shaped fold, b) butterfly diagram (according to Johnson, 2000): Φ – angle of internal friction; other symbols as in Fig. 2a.

4. Results

4.1. Kink fold geometry

We found similar kink folds in both studied mica schist belts (SKSB and SPSB) in the northern part of KIM (Fig. 1), suggesting that these are penetrative structures formed throughout the analyzed area. The most frequent and best developed examples can be observed in mica schists and leptinites of the SKSB (farther from the Karkonosze Granite), whereas in hornfels of the SPSB (closer to the intrusion) the kink folds are significantly less frequent and usually only poorly preserved. Thus, the spatial relation between the folds and the Karkonosze Granite can be noticed.

Kink folds of monoclinal geometry, recorded in all the sites studied, predominate in the study area, whereas conjugate forms, both symmetrical and asymmetrical, were observed only at sites 2, 6, 7, 8, 9, 10, and 13 (see Figs. 3, S1 and S2). These are usually small mesoscale structures. In most of the studied kink folds, the outer limbs are long and dip gently, whereas the inner limbs (kink bands) are steep and narrow, with widths varying from <1 to ~20 cm. Monoclinal structures present both geometries: S-shaped and, more commonly, Z-shaped. The ultimate locking angle of Z-shaped folds (θ_{ULZ}) varies from −40 to −65°, of S-shaped folds (θ_{ULS}) from 40 to 60° (Figs. 3, S1 and S2). Similar values of ultimate locking angles were calculated for conjugate kink folds (Figs. 3, S1 and S2).

The observed kink folds exhibit wide variations in the spatial orientation of outer and inner limbs, fold axes, and axial surfaces (Figs. 3, S1 and S2). Nevertheless, based on the variations in spatial orientation of kink folds, and analyses of their superposition observed in the field, two generations of fold structures can be defined (Fig. 4). Younger folds clearly deform and overprint the orientation of the fold axes of older structures, as evidenced on the photograph (Fig. 4). Clear interferences of studied kink bands with older fold structures were observed in the field but are beyond the scope of this manuscript (see Gaidzik and Żaba, 2017). The older structures trend NW–SE, plunging gently to moderately towards the north, northwest (outside of the Karkonosze Granite), and were observed mainly at sites 1, 4, 6, 7, 10, and 13 (Fig. S1). The younger kink folds trend east-west and plunge at low angles towards E, and were recorded at sites 2, 3, 5, 8, 9, 11, 12, and 13 (Fig. S2).

4.2. Stress and strain analysis

The angle of internal friction (Φ) calculated for conjugate kink folds based on the butterfly diagram analysis varies between 35 and 45°, but most commonly equals 40° (Figs. S1 and S2). Thus, we used $\Phi = 40°$ for the analysis of butterfly diagrams of monoclinal kink folds. The calculated inclination angles (β) for both conjugate and monoclinal kink folds are usually relatively small (<15°), suggesting that the maximum principal stress axis (σ_1) was characterized by an orientation similar to that of the anisotropy plane in the outer limbs. The results of butterfly diagram analysis for selected kink folds from all studied sites, divided into two generations, are presented in the supplementary materials (Figs. S1 and S2) along with the main parameters used in the analysis and sketches of kink folds.

Shortening and stretching directions vary significantly, along with the spatial orientation of the main principal stress axes (σ_1, σ_2, and σ_3) calculated for structures of different generations (Fig. 5a). Older kink folds were developed under west–east-directed shortening (Fig. 5b). The spatial orientation of the maximum compressional stress axis (σ_1), calculated using conjugate kink folds, varies slightly from WSW–ENE (sites 7, 10, and 13) to west–east (site 6; Fig. 5a).

Gentle to steep shortening, rotating from NNW–SSE in the western part of the study area (site 8) to NNE–SSW in the eastern part (sites 2, 3, 5, and 11; Fig. 5b), produced kink folds of the younger generation. The spatial orientations of the σ_1 axis, calculated using conjugate folds, show gentle inclination angles, whereas those calculated using monocline structures indicate a much steeper σ_1 axis (Figs. 5a and S2).

Fig. 1. a) Tectonic setting of the Sudetes and of the studied area (red rectangle) in the Variscan Belt (according to Mazur et al., 2006); b) Geological sketch map of KIM with the location of the study area (black rectangle) (modified after Kryza and Mazur, 1995); c) WNW–ESE geological cross section through KIM (after Żelaźniewicz and Aleksandrowski, 2008); d) location of the field sites (rectangles 1–13) within the geological sketch of the study area; sites located in SPSB: 1) Zwalisko Mt.; 2) Wysoki Kamień Mt.; 3) Zbójnickie Skały, pyrite mine; 4) Zbójnickie Skały, eastern area; 5) Mniszy Las; sites located in SKSB: 6) Czerniawa Zdrój, cave; 7) Czerniawa Zdrój, Czerniawska Kopa Mt.; 8) Czerniawa Zdrój, Ulicko, Czerniawski Las; 9) Świeradów Zdrój, Zajęcznik Mt.; 10) Świeradów Zdrój, Jerzy quarry; 11) Świeradów Zdrój, Łęczyna; 12) Kotlina, near ruins of military centre; 13) Gierczyn, Łyszczyk Mt. Sites with conjugate kink folds are marked in green, whereas those with monoclinal structures are marked in orange.

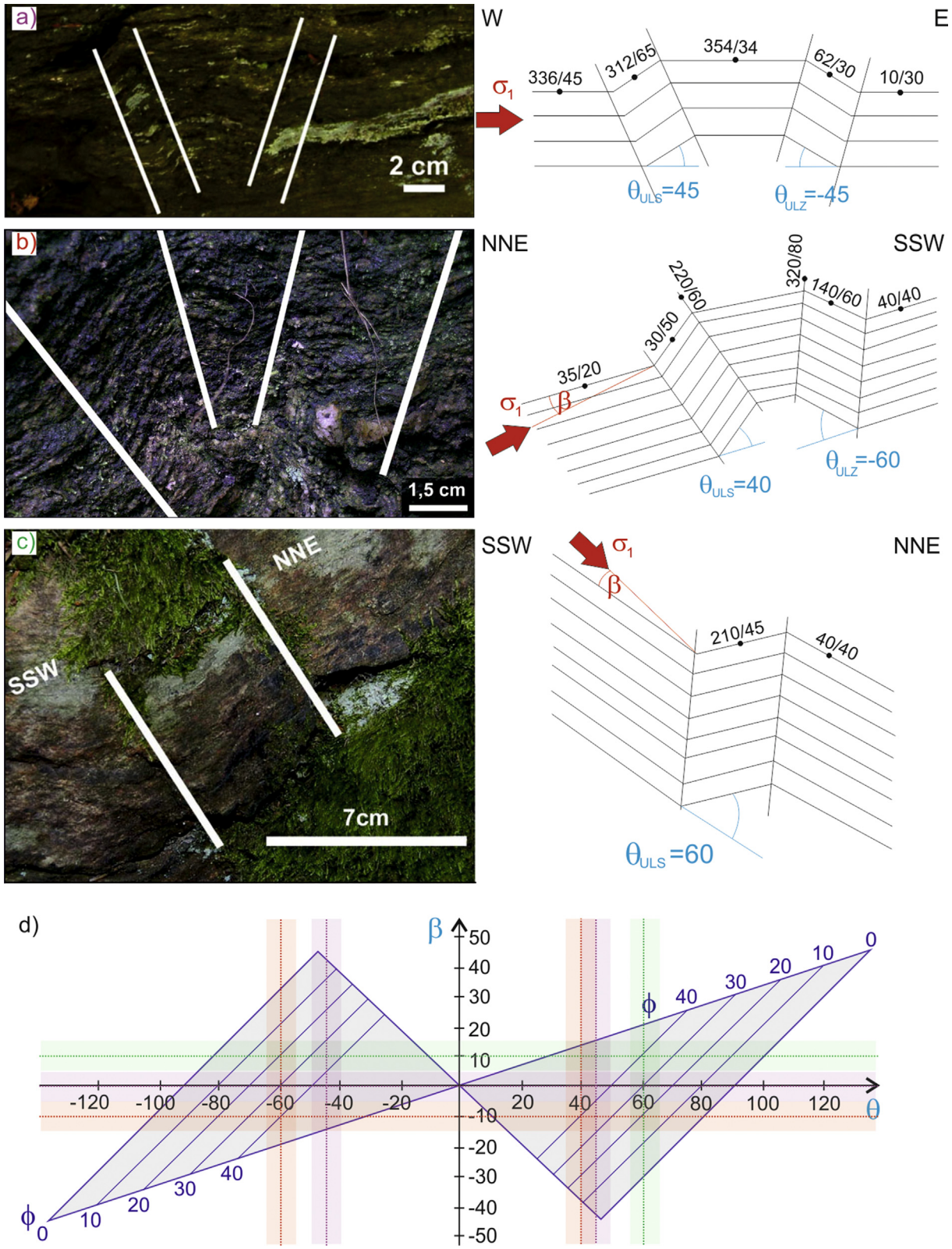

Fig. 3. Examples of kink folds observed in the field (photographs and sketch with main parameters): a – symmetrical conjugate kink fold in mica-schist of the Stara Kamienica belt (site 10 in Fig. 1); b –asymmetrical conjugate kink fold in hornfels of the Szklarska Poręba belt (point 2 in Fig. 1); c – monoclinal kink fold in hornfels of the Szklarska Poręba belt (site 3 in Fig. 1); d – butterfly diagram for kink folds presented in Fig. 3a–c with error bars.

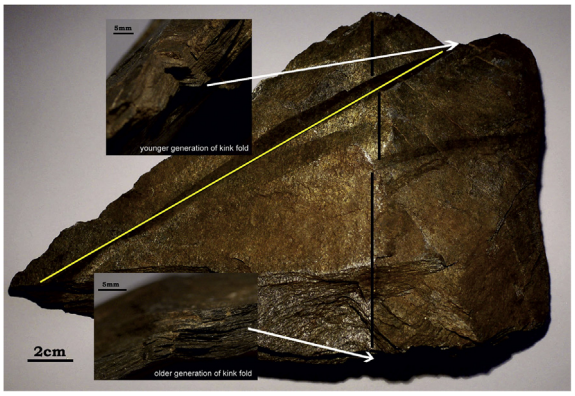

Fig. 4. Superposition of two generations of kink folds in mica-schist of the Stara Kamienica schist belt (site 13 in Fig. 1). The solid black line marks the fold axis of the older generation of kink folds, whereas solid yellow line marks the fold axis of the younger one.

5. Discussion

5.1. Occurrence of kink folds

We found two generations of kink folds in the northern metamorphic envelope of the Karkonosze Granite; each developed differently, depending on the distance of the fold from the granitoid body, i.e. the farther from the intrusion, the more frequent and better developed the kink structures. This might suggest that the studied kink folds are older than the granitoid batholith (i.e. pre-intrusion structures), and consequently were significantly "erased" and "overprinted" as a result of the transformation of mica schists to hornfels on contact with the magmatic body. This may explain the much lower frequency of kink folds in the SPSB, built of hornfels, in comparison with the SKSB, where mica schists mainly occur. In that case, kink folds would be formed before the Variscan intrusion (312–320 Ma; e.g., Kryza et al., 2014; Kusiak et al., 2014; Žák et al., 2013). This agrees with M.P. Mierzejewski (2007), who postulated that all of the identified fold structures were formed prior to the emplacement of the Karkonosze Granite, since they are absent in granites, and commonly overprinted by the contact and structural aureole related to this magmatic body. However, based on the spatial relation between studied folds and the intrusion, these could be also coeval (i.e. synintrusion structures). In that case, the difference in their development would be related with variations in lithology caused by the thermal influence of the Karkonosze Granite, i.e. better developed and more frequent structures in mica schists, and much more limited in hornfels.

The existence of two generations of kink folds was recognized in the field using superposition analysis (Fig. 4) and corroborated by significantly different orientation of the principal stress and strain axes (Fig. 5) calculated for structures of both generations. Two generations of kink folds were also recognized by previous studies, which analyzed the evolution of folds throughout the area (Gaidzik and Żaba, 2017; Żaba, 1984a; Żaba and Kuzak, 1988) or exclusively in the SPSB (Krzykowska, 2007). The results obtained in this study using both methods for conjugate kink folds are similar, proving the reliability of the results obtained by the butterfly diagram analysis used for monoclinal kink folds. In these cases, because of the absence of a second conjugate axial surface, we were not able to calculate the orientation of the principal stress axes using structural diagrams. Nevertheless, our study shows that butterfly diagram analysis (Johnson, 2000) applied to monoclinal kink folds, yields reliable results, especially when calibrated using the internal friction angle (Φ) calculated for the conjugate structures.

5.2. Age and regional implications

The two generations of kink folds analyzed in this study refer to the youngest fold structures observed in the metamorphic rocks of the northern part of KIM (Gaidzik and Żaba, 2017; Jeřábek et al., 2016; Żaba, 1984a; Żaba and Kuzak, 1988). They deform flexural-slip and flow folds of older generations and are followed only by faults, fractures, and joints. Some studies conducted in the southern part of KIM recorded similar kink structures (Gaidzik, 2011; Gaidzik and Żaba, 2017; Jeřábek et al., 2016), whereas others describe only older folds, without any information on kink bands (Žáčková et al., 2010).

We recorded significantly different orientations of principal stress and strain axes for two distinct kink folds (Fig. 5). The older structures (referred as F_4; see Gaidzik and Żaba, 2017) were developed under sublatitudinal horizontal compression (maximum principal stress axis σ_1) (Fig. 5b). Subsequent rotation caused by the doming related to the emplacement of the Karkonosze Granite produced gentle to moderate plunging of the fold axis towards the north, northwest, i.e. outside of the intrusion. However, because the rotation axis was generally perpendicular to the fold axis, it resulted only in fold tilting to the north, i.e. outside of the intrusion. Thus, it did not change the calculated trend of the σ_1 axis, only the plunge of the other stress axes. The younger structures (F_5) were produced by gentle-to-steep sublongitudinal compression (Fig. 5b). These structures were probably formed by north–south compression during the doming of the Karkonosze Granite. From the previous discussion, we know that the studied folds predate or are coeval with the heating and consequent transformation of mica schist into hornfels on contact with the Karkonosze intrusion. The near-horizontal orientation of the σ_1 axis calculated for F_4 folds (Fig. 5) excludes their genetic relation to pressure exerted by the intruding Karkonosze Granite. However, the steeper oriented compression calculated for F_5 kink folds suggests their temporal relation with the Karkonosze Granite.

Thus, we believe that the formation of F_4 kink folds as a result of west–east compression took place in the Early Carboniferous and predated the Karkonosze Granite emplacement (Fig. 6). These folds may have been related to the terminal stages of Late Devonian–Early Carboniferous deformation D_1 in the KIM, identified by Mazur (1995) and resulting in northwest-directed thrusting of the metamorphic envelope. Some studies (Dziemiańczuk and Dziemiańczuk, 1982; Jeřábek et al., 2016) suggest even that at least some of the F_4 kink bands are actually pre-F_3

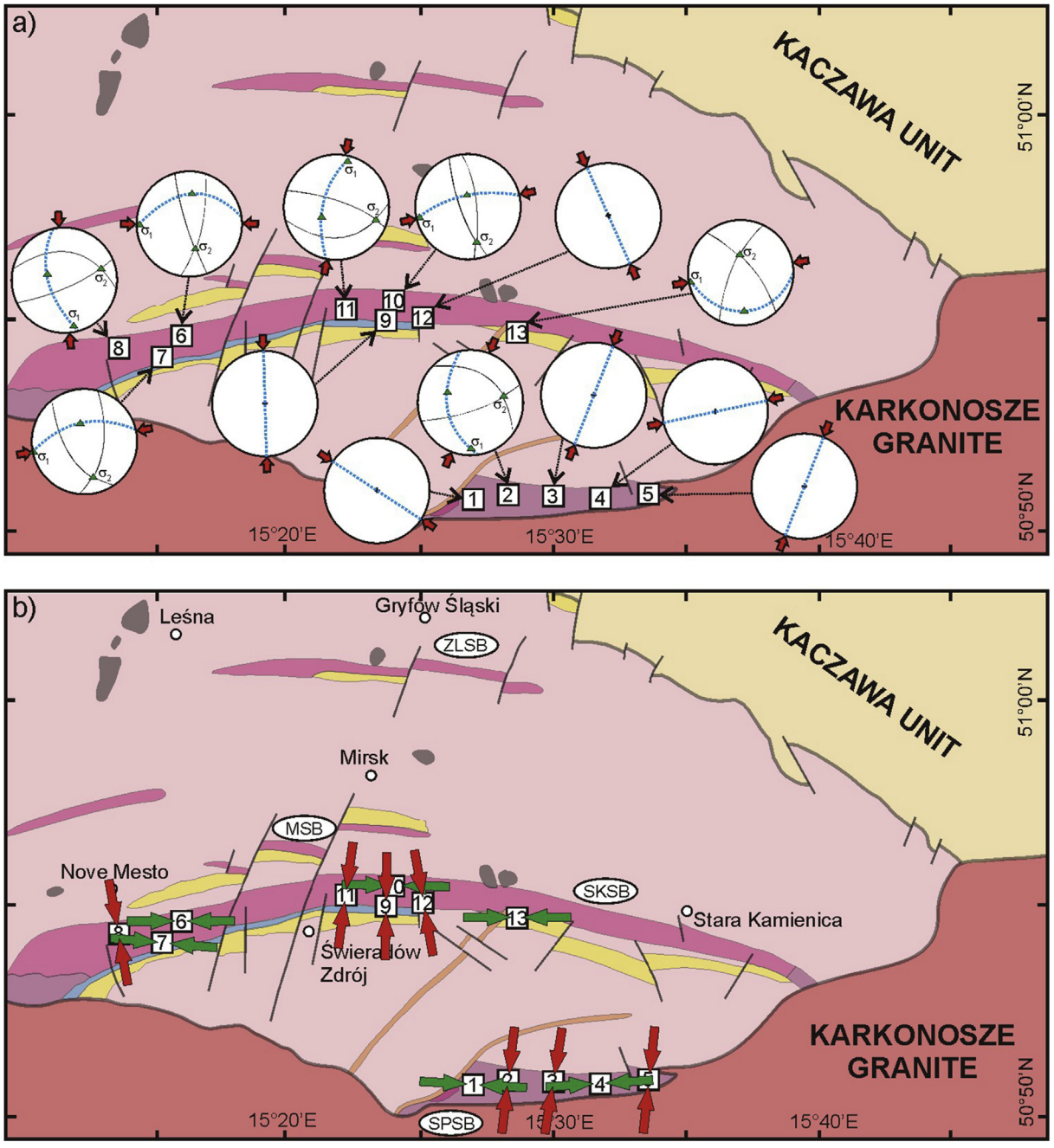

Fig. 5. a – Lateral variations of the orientation of principal stress axes calculated for the observed kink folds in the Izera–Kowary Unit; $\sigma_1 > \sigma_2 > \sigma_3$ – principal stress axes; red arrow – direction of sub-horizontal shortening; b – lateral variations in the direction of sub-horizontal shortening between kink folds of the older (green arrows) and younger (red arrows) generations. For key to colors, see Fig. 1.

structures strictly related with the main phases of the Late Devonian thrusting. This finding confirms that they have to be pre-intrusion structures.

The formation of F_5 kink folds was probably related to the latest stage of the Variscan Carboniferous north–south compression, i.e. Westphalian C (304–313 Ma; Gradstein et al., 2012) and the emplacement and subsequent doming of the Karkonosze Granite, as indicated by gentle-to-steeply inclined σ_1 axis (Fig. 6). Synchronous dextral displacements were observed along the Intra-Sudetic Fault (Aleksandrowski et al., 1997). However, it is believed that they ceased before the emplacement of the Karkonosze Granite, since granites on the contact with the fault are unaffected by fault-related dextral shearing (Aleksandrowski et al., 1997). Dextral displacements observed along other major NW–SE trending faults in the

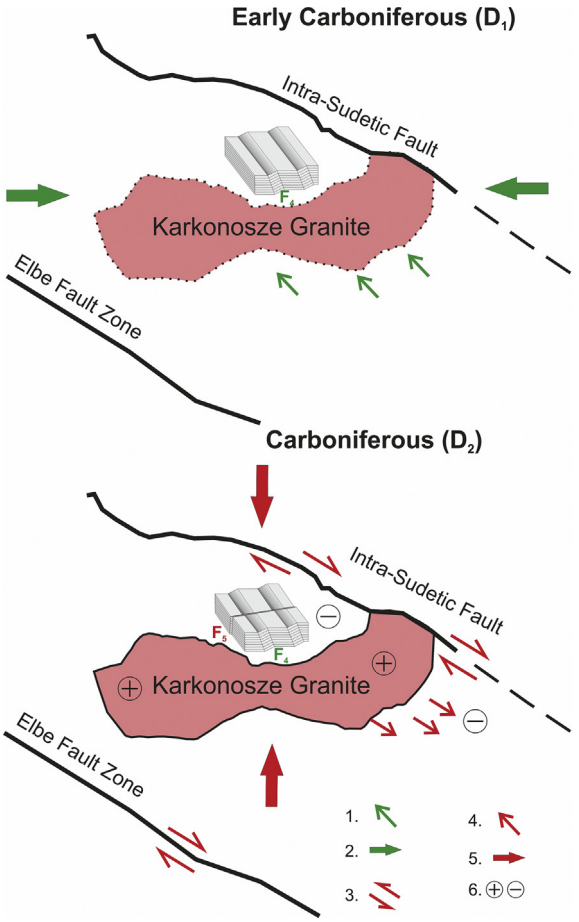

Fig. 6. Relationship of recorded kink fold generations (F_4 and F_5) to regional deformations (D_1 and D_2; according to Mazur, 1995): 1 – northwest thrusting in the Karkonosze–Izera Massif; 2 – west–east compression during the D_1 event; 3 – dextral displacements on ISF (according to Aleksandrowski et al., 1997); 4 – ESE extensional collapse in KIM; 5 – north–south compression; 6 – relative uplift and subsidence related to doming of the Karkonosze Granite. Sketch not to scale.

northern part of the Bohemian Massif, such as the Elbe and Middle Odra Faults (Aleksandrowski, 1995; Aleksandrowski et al., 1997) corroborate north–south compression. The formation of F_5 folds and the dextral activity on the ISF seems to be related to the D_2 event in the KIM and subsequent ESE-directed gravitational collapse that followed the nappe stocking (Aleksandrowski and Mazur, 2002; Aleksandrowski et al., 1997; Diot et al., 1994; Mazur, 1995; Mazur and Aleksandrowski, 2001; Mazur et al., 2006). The recorded north–south compression and dextral activity along major NW–SE-trending faults, along with the subsequent extensional event, agree with the symmetric and asymmetric models of the Karkonosze Granite emplacement (Diot et al., 1994).

The studied structures terminate the Variscan subduction-exhumation processes in the Bohemian Massif usually correlated with F_1 to F_3 folds (e.g., Jeřábek et al., 2016). Whereas F_4 structures could have been formed at the late stages of convergence as a result of shortening in the accretionary wedge, probably related with change from continental subduction to continental collision, younger structures F_5 the most probably the result of north–south shortening commonly recorded in Bohemian Massif (e.g., Aleksandrowski, 1995; Aleksandrowski et al., 1997; Jeřábek et al., 2016) and the Karkonosze Granite emplacement and doming. Younger deformation observed in KIM are connected with brittle deformations.

5. Conclusions

1. Based on our results, we suggest the existence of two generations of kink folds in the northern metamorphic envelope of the Karkonosze Granite.
2. We recorded significantly different orientations of the principal stress and strain axes for two generations of kink fold structures. The older folds were developed under sublatitudinal horizontal compression (maximum principal stress axis σ_1), whereas the younger folds were produced by a gently to steeply north–south-trending compression axis.
3. Older kink folds were produced prior to the Karkonosze Granite intrusion emplacement (~312–320 Ma), related to the terminal, Early Carboniferous stages of west–east compression, probably during continental collision. Younger kink bands were produced in the latest stage of the Variscan Carboniferous north–south compression, and consequent emplacement of the Karkonosze Granite and its doming.
4. We obtained similar orientation of principal stress and strain axes for the conjugate kink folds using two different methods: 1) the traditional method, incorporating structural diagrams, and 2) butterfly diagram analysis, proving the correctness and reliability of both methods.
5. The results obtained in this study prove that butterfly diagram analysis, when applied to monoclinal kink folds, yields reliable results, especially when calibrated using the internal friction angle (Φ) calculated for the conjugate structures.

Acknowledgements

Funding was provided by grant N307 244339 (State Committee for Scientific Research, Poland). The publication was partially financed from the funds of the Leading National Research Center (KNOW) received by the Center for Polar Studies of the University of Silesia, Poland.

Appendix A. Supplementary data

Supplementary data to this article can be found online at https://doi.org/10.1016/j.crte.2019.04.003.

References

Aleksandrowski, P., 1995. The significance of major strike-slip displacements in the development of Variscan structure of the Sudetes, SW Poland. Przegl. Geol. 43, 745–754.

Aleksandrowski, P., Mazur, S., 2002. Collage tectonics in the northeastern part of the Variscan belt: the Sudetes, Bohemian massif. In: Winchester, J.A., Pharaoh, T.C., Verniers, J. (Eds.), Palaeozoic

Amalgamation of Central Europe. Geol. Soc. London Special Publications 201, pp. 237–277.
Aleksandrowski, P., Kryza, R., Mazur, S., Żaba, J., 1997. Kinematic data on major Variscan strike-slip faults and shear zones in the Polish Sudetes, northeast Bohemian massif. Geol. Mag. 134 (5), 727–739.
Anderson, T.B., 1974. The relationship between kink-bands and shear fractures in the experimental deformation of slate. J. Geol. Soc. London 130, 367–382.
Barton, N., Choubey, V., 1977. The shear strength of rock joints in theory and practice. Rock Mech. 10, 1–54.
Behr, H.J., 1983. Intracrustal and subcrustal thrust-tectonics at the northern margin of the Bohemian Massif. In: Martin, H., Eder, F.W. (Eds.), Intracontinental Fold Belts. Springer, Berlin, Heidelberg, pp. 365–403.
Borkowska, M., 1966. Petrography of the Karkonosze granite. Geol. Sudetica 2, 7–107.
Borkowska, M., Hameurt, J., Vidal, P., 1980. Origin and age of Izera granite and Rumburk granite in the Western Sudetes. Acta Geol. Pol. 30 (2), 121–146.
Chaloupský, J., 1989. Geology of the Krkonoše and Jizerské Hory Mts. Ust. Ústav Geol., Praha, 288 p.
Collier, M., 1978. Ultimate locking angels for conjugate and monoclinal kink bands. Tectonophysics 48, 1–6.
Czapliński, W., 1998. Orthogneisses and metapelites from a polyphase tectonic zone – mezostructural versus microstructural evidence: an example from Czerniawa Zdrój section (Izera-Karkonosze Block, West Sudetes). Geol. Sudetica 31, 93–104.
Dewey, J.F., 1965. Nature and origin of kink bands. Tectonophysics 1 (6), 459–494.
Diot, H., Mazur, S., Couturie, J.P., 1994. Magmatic Structures in the Karkonosze Granite and Their Relation to Tectonic Structures in the Eastern Metamorphic Cover. Abstracts of the Igneous Activity and Metamorphic Evolution of the Sudetes Area. Uniwersytet Wrocławski, Wrocław, pp. 36–39, 12-15.05.1994.
Dunham, R.E., Crider, J.G., 2012. Geometric curvature analysis of intersecting kink bands: a new perspective on the 3D geometry of kink folds. J. Struct. Geol. 37, 236–247. https://doi.org/10.1016/j.jsg.2012.01.003.
Dziemiańczuk, E., Dziemiańczuk, K., 1982. Structural development of micaceous schists of the Pasmo Kamienickie renge between Czerniawa and Rębiszów. Geol. Q. 26 (1), 13–43.
Franke, W., Żelaźniewicz, A., 2000. The eastern termination of the Variscides: terrane correlation and kinematic evolution. In: Franke, W., Haak, V., Oncken, O., Tanner, D. (Eds.), Orogenic Processes: Quantification and Modelling in the Variscan Belt. Geol. Soc. London, Special Publications 179, pp. 63–86.
Gaidzik, K., 2011. Tektonika Południowej Strefy Kontaktowej Masywu Granitoidowego Karkonoszy W Rejonie Karpacza. PhD thesis. University of Silesia, Sosnowiec. unpublished manuscript.
Gaidzik, K., Żaba, J., 2017. Comparison of fold deformation sequences in the northern and southern metamorphic cover of the Karkonosze granitoids. Przegl. Geol. 65 (12), 1548–1554.
Gradstein, F.M., Ogg, J.G., Schmitz, M., Ogg, G. (Eds.), 2012. The Geologic Time Scale 2012. Elsevier, China, 1144 p.
Honea, E., Johnson, A.M., 1976. Development of sinusoidal and kink folds in multilayers confined by rigid boundaries. Tectonophysics 30, 197–239.
Jeřábek, P., Konopásek, J., Žáčková, E., 2016. Two-stage exhumation of subducted Saxothuringian continental crust records underplating in the subduction channel and collisional forced folding (Krkonoše-Jizera Mts., Bohemian Massif). J. Struct. Geol. 89, 214–229. https://doi.org/10.1016/j.jsg.2016.06.008.
Johnson, A.M., 1977. Styles of Folding. Mechanics and Mechanisms of Folding of Natural Elastic. Elsevier, Amsterdam, New York.
Johnson, K.M., 2000. Methods of Structural Analysis of the Spotted Wolf Section of the San Rafael Monocline, Utah. M.S. thesis. Purdure University, Indiana. unpublished manuscript.
Johnson, K.M., Manuszak, J.D., 2001. How to Analyze Kink Folds: Filed Examples from the Eastern Alaska Range and San Rafal Swell, Utah. www.purdue.edu.
Julivert, M., Soldevila, J., 1998. Small-scale structures formed during progressive shortening and subsequent collapse in the Navia-Alto Sil slate belt (Hercynian fold belt, NW Spain). J. Struct. Geol. 20 (4), 447–458. https://doi.org/10.1016/S0191-8141(97)00107-7.
Kirschner, D.L., Teixell, A., 1996. Three-dimensional geometry of kink bands in slates and its relationship with finite strain. Tectonophysics 262, 195–211. https://doi.org/10.1016/0040-1951(96)00003-0.
Kröner, A., Jaeckel, P., Hegner, E., Opletal, M., 2001. Single zircon ages and whole-rock Nd isotopic systematics of early Palaeozoic granitoid gneisses from the Czech and Polish Sudetes (Jizerské hory, Krkonoše mountains and Orlice–Sněžník complex). Int. J. Earth Sci. 90 (2), 304–324. https://doi.org/10.1007/s005310000139.
Kryza, R., Schaltegger, U., Oberc-Dziedzic, T., Pin, C., Ovtcharova, M., 2014. Geochronology of a composite granitoid pluton: a high-precision ID-TIMS U–Pb zircon study of the Variscan Karkonosze Granite (SW Poland). Int. J. Earth Sci. 103 (3), 683–696. https://doi.org/10.1007/s00531-013-0995-0.
Kryza, R., Mazur, S., 1995. Contrasting metamorphic paths in the eastern margin of the Karkonosze-Izera Block, SW Poland. N. Jb. Miner. Abh. 169 (2), 157–192.
Krzykowska, R., 2007. King folds in Szklarska Poręba schist belt (Izera Mountains) – application of butterfly diagram in structural analysis. Prace Naukowe Instytutu Górnictwa Politechniki Wrocławskiej 120 (49), 161–169.
Kusiak, M.A., Williams, I.S., Dunkley, D.J., Konečny, P., Słaby, E., Martin, H., 2014. Monazite to the rescue: U–Th–Pb dating of the intrusive history of the composite Karkonosze pluton, Bohemian Massif. Chem. Geol. 364, 76–92. https://doi.org/10.1016/j.chemgeo.2013.11.016.
MacKenzie, D., Craw, D., Cooley, M., Fleming, A., 2010. Lithogeochemical localisation of disseminated gold in the White River area, Yukon, Canada. Miner. Depos. 45 (7), 683–705. https://doi.org/10.1007/s00126-010-0301-z.
Majka, J., Mazur, S., Kośmińska, K., Dudek, K., Klonowska, I., 2016. Pressure–temperature estimates of the blueschists from the Kopina Mt., northern Bohemian Massif, Poland–constraints on subduction of the Saxothuringian continental margin. Eur. J. Mineral. 28 (6), 1047–1057. https://doi.org/10.1127/ejm/2016/0028-2601.
Mazur, S., 1995. Structural and metamorphic evolution of the country rocks at the eastern contact of the Karkonosze granite in the southern Rudawy Janowickie Mts and Lasocki Range. Geol. Sudetica 29, 31–98.
Mazur, S., Aleksandrowski, P., 2001. The Tepla(?)/Saxothuringian suture in the Karkonosze-Izera massif, western Sudetes, central European Variscides. Int. J. Earth Sci. 90, 341–360. https://doi.org/10.1007/s005310000146.
Mazur, S., Kryza, R., 1996. Superimposed compressional and extensional tectonics in the Karkonosze-Izera Block, NE Bohemian massif. In: Oncken, O., Janssen, D. (Eds.), Europe and Other Regions. Basement Tectonics 11, pp. 51–66.
Mazur, S., Aleksandrowski, P., Kryza, R., Oberc-Dziedzic, T., 2006. The Variscan orogen in Poland. Geol. Q. 50 (1), 89–118.
Mierzejewski, M.P., 2007. A general view on the Karkonosze granite. In: Kozłowski, A., Wiszniewska, J. (Eds.), Granitoids in Poland. Archivum Mineralogiae Monograph 1, pp. 111–122.
Oberc-Dziedzic, T., Kryza, R., Mochnacka, K., Larionov, A., 2010. Ordovician passive continental margin magmatism in the Central-European Variscides: U–Pb zircon data from the SE part of the Karkonosze-Izera Massif, Sudetes, SW Poland. Int. J. Earth Sci. 99 (1), 27–46. https://doi.org/10.1007/s00531-008-0382-4.
Oliver, G.J.H., Corfu, F., Krogh, T.E., 1993. U-Pb ages from SW Poland; evidence for a Caledonian suture zone between Baltica and Gondwana. J. Geol. Soc., London 150, 355–369. https://doi.org/10.1144/gsjgs.150.2.0355.
Ramsay, J.G., Huber, M.I., 1987. The Techniques of Modern Structural Geology, vol. 2. Academic Press.
Reches, Z., Johnson, K.M., 1976. Asymmetric folding and monocline kinking. Tectonophysics 35, 295–340.
Rubinkiewicz, J., 2005. Kink folds and kink bands – geometry, conditions of nucleation, interpretation – an example from Outer Carpathian flysch. Przegl. Geol. 53 (11), 1040–1046.
Seston, R., Winchester, J.A., Piasecki, M.A.A., Crowley, Q.G., Floyd, P.A., 2000. A structural model for the western-central Sudetes: a deformed stack of Variscan thrust sheets. J. Geol. Soc., London 157, 1155–1167.
Verbeek, E.R., 1978. Kink bands in the Somport slates, west-central Pyrenees, France and Spain. Geol. Soc. Am. Bull. 89, 814–824.
Żaba, J., 1979. The northern contact of the Karkonosze granite with its country rocks in the vicinity of Szklarska Poręba, western Sudetes. Geol. Sudetica 14 (2), 47–74.
Żaba, J., 1984a. Stosunek waryscyjskiego granitoidu Karkonoszy do metamorfiku północnej osłony oraz tektonika fałdowa pasm łupkowych Szklarskiej Poręby i Starej Kamienicy (krystalinik izerski). In: Zagadnienia Tektoniki Krystaliniku Izersko – Łużyckiego. Terenowa Konferencja Naukowa, Jelenia Góra – Gorlitz, 27- 28 Maja 1984. Uniwersytet Śląski, Katowice, pp. 7–72.

Żaba, J., 1984b. Genesis and metamorphic evolution of gneisses and granitoids of the Izerski Stóg massif, Western Sudetes. Geol. Sudetica 19 (2), 89–190.

Żaba, J., Kuzak, R., 1988. Structure of the middle part of the Szklarska Poręba slate Range. Izera Mts. Geol. Q. 32 (3–4), 635–653.

Žáčková, E., Konopásek, J., Jeřábek, P., Finger, F., Košler, J., 2010. Early Carboniferous blueschist facies metamorphism in metapelites of the West Sudetes (northern Saxothuringian domain, Bohemian massif). J. Metamorph. Geol. 28 (4), 361–379. https://doi.org/10.1111/j.1525-1314.2010.00869.x.

Žák, J., Verner, K., Sláma, J., Kachlík, V., Chlupáčová, M., 2013. Multistage magma emplacement and progressive strain accumulation in the shallow-level Krkonoše-Jizera plutonic complex, Bohemian Massif. Tectonics 32 (5), 1493–1512. https://doi.org/10.1002/tect.20088.

Żelaźniewicz, A., Aleksandrowski, P., 2008. Tectonic subdivision of Poland: southwestern Poland. Przegl. Geol. 56 (10), 904–911.